# Rheology and composition of citrus fiber

Brock Lundberg [a,b,*], Xuejun Pan [a], Andre White [c], Hoa Chau [c], Arland Hotchkiss [c]

[a] Department of Biological Systems Engineering, University of Wisconsin-Madison, 460 Henry Mall, Madison, WI 53706, USA
[b] Fiberstar, Inc., 713 Saint Croix Street, River Falls, WI 54022, USA
[c] U.S. Department of Agriculture, Agricultural Research Service, Eastern Regional Research Center, Dairy and Functional Foods Research Unit, 600 E Mermaid Lane, Wyndmoor, PA 19038, USA

## ARTICLE INFO

## ABSTRACT

While fibrous byproducts are abundant, using them in food products to improve food nutrition and quality without degrading taste or texture can be challenging. Citrus fiber has been shown to have high water holding capacity and apparent viscosity. However, to better incorporate citrus fiber into foods, their rheological properties, and composition, need to be better understood. Pectin was found to be 42% of the composition of the citrus fiber evaluated in this study. The rheological properties of citrus fiber solutions were clearly non Newtonian and the type of model that best fit the citrus fiber varied depending on its particle size. Particle size of citrus fiber also significantly changed the apparent viscosity of their solutions. As citrus fibers hydrate, the fibers swell, which was illustrated by microscopic imaging.

© 2013 Elsevier Ltd. All rights reserved.

## 1. Introduction

Appearance, flavor, texture, and nutrition are known factors that play a role in creating high quality foods (Bourne, 1992). Although there are many definitions, texture is defined by the International Organization for Standardization as properties that encompass all the rheological and structural attributes of a food product that are perceptible by mechanical, tactile, and when appropriate, visual and auditory receptors. Thus, the assessment of texture begins when a consumer opens a food product container, handles it, and prepares it, all the way through consuming the product. Consumer textural preference is based on the attributes at each point in the process starting when the consumer first sees the product through the point when the product is consumed and the food product undergoes many changes in that process. Therefore, producing food products with favorable textural qualities has many dynamic aspects and can be complex (Borwankar, 1992).

Because fibrous plant cell walls typically play an important role in determining the quality characteristics of the foods that they go into, there is further need to understand not only how they function but also why fibrous materials function the way they do (Van Buren, 1979). Important factors determining food texture are composition and rheological properties (Bourne, 1992). Thus,

knowing information related to the rheology, function, and composition of ingredients is important for a food product engineer as well as quality control, process control, and design of process equipment (Saravacos, 1970; Ofoli et al., 1987).

One method used to enhance the functionality of fibrous materials, e.g. food processing byproducts, is to expand their internal surface area, which increases water binding capacity and/or apparent viscosity so they are better suited to improve the nutritional and/or quality of foods (Turbak et al., 1983). Ruan et al. (1996) made a product similar to microfibrillated cellulose, called highly refined cellulose, utilizing agricultural residues and food processing byproducts. Citrus fiber also has high internal surface area, water holding capacity and apparent viscosity (Lundberg, 2005). Its high water holding capacity, ability to increase yields and retain moisture means that citrus fiber has many food applications in baked products, meats, dairy products, sauces and dressings. Moreover, because of the neutral color, taste, and odor, processed citrus fiber make products suitable for many applications where other fibrous products would otherwise not be considered (Garau et al., 2007; Grigelmo-Miguel and Martin-Belloso, 1999). One of the unique challenges of citrus fiber is how to dry it while maintaining functional properties upon rehydration (Braddock, 1999). Although overcoming the challenge of producing citrus fiber in a dried form while maintaining functional properties has been overcome, more research is needed to better understand its functionality. Improving this understanding will not only expand the ability to utilize plant cell walls in more applications, but also it will help create healthier foods, which is an underlying goal of

---

* Corresponding author at: Department of Biological Systems Engineering, University of Wisconsin-Madison, 460 Henry Mall, Madison, WI 53706, USA. Tel.: +1 6512710328.
E-mail addresses: brocklundberg3@gmail.com, b.lundberg@fiberstar.net (B. Lundberg).

this study. There is also a lack of information documenting the rheology of citrus fiber and the effect of its composition on the rheology. Knowing more about the rheology of citrus fiber will enable manufacturers to be better informed in designing as well as manufacturing food products that contain citrus fiber ingredients. The objective of this research is to study the composition and rheology of citrus fibers to gain an understanding of how to better apply the product in food applications.

## 2. Materials and methods

### 2.1. Raw materials

The citrus fiber studied in this project was obtained from orange (*Citrus sinensis*) pulp or juice vesicles, which is a byproduct of orange juice production. The production process and source of citrus fiber were consistent with those previously described by Fiberstar, Inc. (River Falls, WI) (Lundberg, 2005). Chemicals used in this study were purchased from Sigma–Aldrich (St. Louis, MO) and used as received.

### 2.2. Compositional analysis

Protein was measured using the Dumas method as outlined in AOAC International Method 992.15, where the sample was combusted and nitrogen content measured. Protein was calculated from the nitrogen content by a timing factor of 6.25. Total fat was measured following AOAC method 996.06, where lipids were extracted and quantified using capillary column gas chromatography. Moisture was determined by heating the sample in a vacuum oven for 18 h following AOAC method 925.09. Total carbohydrates were found by subtracting fat, protein, ash and moisture from 100%.

Cellulose and hemicellulose were quantified after acid hydrolysis, and the sugars released in the hydrolysate were determined using the HPLC method described in the Laboratory Analytical Procedure NREL LAB method #002 (Sluiter et al., 2006). From the HPLC data, cellulose was determined by counting the weight of glucan measured. Hemicellulose was calculated by adding xylan, glucomannan, 36% of the galactan and 9.5% of the arabinan found in the monosaccharides. These percentages of galactan and arabinan were used because they represent the relative amounts previously found in orange pulp as reported by Ting (1970).

For pectin and galacturonic acid (GA) analysis, the degree of esterification (DE), degree of acetylation (DA), and extractable carbohydrate analysis was conducted according to Yoo et al. (2003). Pectin content in the carbohydrate fraction was found by adding the arabinose, galactose, rhamnose, and galacturonic acid found from the monosaccharide analysis using the percentages reported in orange pulp by Ting (1970). For instance, Ting (1970) found that 90% of arabinose, 63.8% of galactose, 99% of galacturonic acid, and 100% of rhamnose made up pectic substances in orange pulp and the remaining amount of each monosaccharide made up hemicellulose. Total pectin in the citrus fiber was calculated by multiplying the pectin content found from the monosaccharide analysis amount by the total extractable carbohydrates as determined by the methods described in Yoo et al. (2003).

### 2.3. Water holding capacity

As a measure of the samples' degree of hydrophilic properties, the water holding capacity was measured following American Association of Cereal Chemists (AACC) Method 56-30, which included centrifuging the sample at 2000*g*, with a minor modification needed to accommodate a high water holding capacity

material. The modified method involved weighing 2.5 g of dry material into the centrifuge tube for the measurement instead of 5.0 g that the standard procedure called for.

### 2.4. Swelling capacity

Swelling capacity, defined as the ratio of the volume occupied when the sample is immersed in excess of water after equilibration to the sample weight, was measured by the method of Raghavendra et al. (2004). To 0.2 g of dry sample placed in a graduated test tube; around 10 mL of water was added to hydrate the sample for 18 h; then the final volume attained by fiber was measured. The swelling capacity was then calculated using the following equation:

$$\text{Swelling Capacity} \left(\frac{\text{mL}}{\text{g}}\right) = \frac{\text{final volume occupied by sample (ml)}}{\text{original sample weight (g)}}$$

(1)

### 2.5. Hydration procedure

To prepare the samples for rheological measurements, dried (4–8% moisture content) samples were blended in water for 3 min in a Waring blender on low speed to begin the hydration process. After blending, they were allowed to sit for 30 min to allow for the solution to come to equilibrium. Unless otherwise mentioned, the citrus fiber samples were hydrated at 3% solids and at room temperature (25 °C).

### 2.6. Rheological measurement

A Brookfield DV-II+ viscometer with cylindrical spindles (Brookfield spindle types: #1 LV, #2 LV CYL, #3 LV CYL, #4 LV) was used for all the rheological work and apparent viscosity measurements. The range of speed varied from 0.5 rpm up to 200 rpm. However, when apparent viscosity measurement was taken, 10 rpm was used. A 250 mL sample at 3% solids and a temperature of 25 °C was used for apparent viscosity measurement unless noted otherwise.

### 2.7. Particle size

Homogenous citrus fiber was ground to different degrees in order to obtain a range of particle sizes. Dynamic light scattering was used for measuring the particle width of the citrus fiber samples. The range of lengths that could be determined using dynamic light scattering is limited to 300 μm; thus, fiber length was determined using laser diffraction with a Microtrac 3500 (Montgomeryville, PA) particle size analyzer. The length and width measurements used in this study are shown in Table 1.

### 2.8. Statistics

Where error bars are shown in the graphs, they were calculated using a t-distribution with a 95% confidence interval and Excel software.

**Table 1**
Fiber width and length measurements for the various samples in this study.

| Sample ID | Width (μm) | Length (μm) |
|-----------|-----------|-------------|
| F33 | 33.6 | 363 |
| F27 | 30.8 | 180 |
| A01 | 27.2 | 76.2 |
| A02 | 19.0 | 41.5 |
| J01 | 11.2 | 12.7 |

## 2.9. Light microscopy

To illustrate the effect of water on the dried fiber structure as they rehydrate, photos of fiber sample "F33" were taken before and after water was added. 0.2 g of the fiber sample was added to a standard microscope slide with a cover slide on top. Using a pipette, 2 mL of water was placed on the edge of the cover slide and allowed to diffuse in via capillary action. A Celestron 1600X LCD digital light microscope at 37. 5× magnification was used for taking the images of the fibers as they hydrated.

## 3. Theory and calculation

### 3.1. Rheology

Because citrus fiber solutions are generally non-Newtonian, the viscosity varies with shear rate. Moreover, shear-thinning behavior is common for fruit purees, so models were selected that would describe this behavior (Steffe, 1996). Yield stress, which is the shear stress that needs to be applied to the solution before it begins to flow, was found using an indirect measurement (Pimenova and Hanley, 2004). The method involves extrapolation of the stress–shear rate data to the $y$ axis, which is the theoretical value of the shear stress. Although yield stress is an extrapolated value in this study, it is in fact an engineering reality (Hartnett and Hu, 1989); thus, models were selected that contain a yield stress component (Hershel–Bulkley, Casson, and Bingham) and compared to a model that does not contain it (Power Law). The methods used to linearize the data for all the flow models (Herschel–Bulkley, Casson, Power Law, and Bingham) used in this project are shown in Table 2. In each model discussed below (other than the Power Law), "$\sigma_o$" is the yield stress value, "$K$" is the consistency index, and "$n$" is the flow behavior index, which is a parameter that determines the shear-thinning nature of the solutions. The Herchel–Bulkley model is a general relationship that can be used to describe the flow behavior of non-Newtonian fluids. Several other models, e.g. Power Law and Bingham, can be considered as special cases of the Herschel–Bulkley model. For instance, when the yield stress component is zero and $0 < n < 1$, the Herschel–Bulkley model becomes the Power Law model with shear thinning behavior (Steffe, 1996). A Bingham plastic material will have a flow behavior index ($n$) of one and a consistency factor greater than zero. The general form of the Herchel–Bulkley model is shown in Eq. (2) below:

Herschel–Bulkley Model

$$\sigma = \sigma_o + K(\dot{\gamma})^n \tag{2}$$

where $K$ is the consistency coefficient, $n$ is the flow behavior index, and $\sigma_o$ is the yield stress, $\sigma$ is the shear stress, and gamma dot is the strain rate.

The Casson flow model, which has a yield stress and describes shear thinning fluids, was selected because it is used frequently to describe solutions that have interacting particles in a pseudo-plastic based solvent (Rao, 1977). The model was originally introduced to predict the flow behavior of pigment-oil suspensions and is based on an interactive behavior of solid and liquid phases

of a two-phase suspension (Casson, 1959). The Casson model has also been used in prior studies to describe the flow behavior of concentrated orange juice (Mizrahi and Berk, 1972) as well as fruit and tomato purees (Charm, 1960). Based on prior studies, the yield stress component as determined from the Casson model has been found to closely match the yield stress as determined by a narrow gap concentric cylinder viscometer (Rao, 1977). The Casson flow model is described below in Eq. (3):

Casson Model

$$\sigma^{0.5} = (\sigma_o)^{0.5} + K(\dot{\gamma})^{0.5} \tag{3}$$

Because the fluids in this project are non-Newtonian, i.e. flow behavior index not being one, the following equation (Eq. (4)) was used to calculate the apparent viscosity ($\eta$) of the fluid. This apparent viscosity was used as the primary measurement of the fluid's behavior in this study.

Apparent viscosity ($\eta$) calculation:

$$\eta = f(\dot{\gamma}) = \frac{K(\dot{\gamma})^n + \sigma_0}{\dot{\gamma}} = K(\dot{\gamma})^{n-1} + \frac{\sigma_o}{\dot{\gamma}} \tag{4}$$

## 4. Results and discussion

### 4.1. Composition of citrus fiber

The basic composition of the citrus fibers evaluated in this study is shown in Table 3. The citrus fibers are mostly composed of carbohydrates, which make up approximately 80% of the total composition. The most prevalent polysaccharides in the citrus fibers are pectin (42.25%) and cellulose (15.95%). Considering the source of the raw material, this is not a surprise and is consistent with others who also report similar amounts of pectin and cellulose in citrus fiber (Braddock, 1983, 1999; Whitaker, 1984). Because of the acidic and therefore charged (e.g. galacturonic acid) nature of the pectin components, it is used in many applications for its apparent viscosity or gelling properties (Willats et al., 2006). Thus, the pectin in the citrus fiber is likely a contributing factor to its functional properties.

Hemicellulose also makes up a significant fraction of the citrus fiber at 10.06% (Table 3). Hemicellulose has high apparent viscosity when it hydrates and has a high water holding capacity because of its branched, generally amorphous, and non-crystalline structure (Wen et al., 1998). Although the chemical composition is different from pectin, hemicellulose is also likely contributing to the citrus fiber's apparent viscosity and water holding capacity.

**Table 2**
Linear regression models for the various flow types evaluated in this study (Steffe, 1996).

| Model | $y$ | $x$ |
|---|---|---|
| Herschel–Bulkley | $\ln(\sigma - \sigma_o)$ | $\ln\dot{\gamma}$ |
| Casson | $\sigma^{0.5}$ | $(\dot{\gamma})^{0.5}$ |
| Power Law | $\ln(\sigma)$ | $\ln\dot{\gamma}$ |
| Bingham | $\sigma$ | $\dot{\gamma}$ |

**Table 3**
Composition of the citrus fiber used in this study.

| Composition | Value | Units | $n^{[a]}$ | Std dev. |
|---|---|---|---|---|
| Total Fat | **1.05** | % | 7 | 0.12 |
| Carbohydrates | **80.73** | % | 7 | 0.92 |
| Cellulose | 15.95 | % | 3 | 0.02 |
| Hemicellulose | 10.06 | % | 3 | 0.15 |
| Pectin | 42.25 | % | 4 | 1.09 |
| Sugars | 7.36 | % | 7 | 2.68 |
| Other | 5.12 | % | | |
| Protein | **8.15** | % | 7 | 0.45 |
| Ash | **2.65** | % | 7 | 0.26 |
| Moisture | **7.42** | % | 7 | 0.73 |
| Total (bold items) | **100.00** | % | | |

[a] Indicates the number of measurements.

### 4.2. Pectin in citrus fiber

Pectin, which is mainly composed of galacturonic acid, rhamnose, arabinose, and galactose monomers, is thought to form a matrix in the citrus plant cell wall that intersperse with cellulose and hemicelluloses (Waldron et al., 2003). The analysis of the monosaccharides (galacturonic acid, arabinose, rhamnose, and galactose) found in pectin fraction of the citrus fiber is shown in Table 4. Approximately half of the pectin was galacturonic acid, which is a monosaccharide known to be partially methyl-esterified. It produces an acidic or negatively charged group depending on the pH, considering the p$K$a of galacturonic acid is 3.5 (Sila et al., 2009). The pectin degree of esterification was measured to have a 58.1% degree of methyl esterification (DM) and 9.8% degree of acetyl esterification (DA), as shown in Table 4. The citrus fiber degree of methyl esterification was lower than typical citrus peel pectin which is in the range of 70–80% (Waldron et al., 2003). In nature, pectin from citrus products is synthesized in a highly methyl-esterified form but maturation and ripening of the fruit reduces the esterification through enzymatic action. The citrus fiber degree of acetylation was higher than values typical for citrus peel pectin. The DA of commercial citrus pectin (Danisco Pectin 1400) was 1.1% using the same methods. The degree of methyl esterification makes a difference in the functionality of pectin – more junction zones and calcium cross linking occur with less esterification. In jams and jellies that include highly esterified pectin cross linking occurs between the homogalacturonic acid backbone by hydrogen bond bridges and hydrophobic forces between methoxyl groups that is promoted by the addition of sucrose (Willats et al., 2006).

The second most abundant pectin monosaccharide present in processed citrus fiber was arabinose (Table 4). This is an important finding because arabinose occurs in the branches of the galacturonic acid backbone, i.e. rhamnogalacturon I and rhamnogalacturon II (Willats et al., 2006). The branching in the galacturonic acid backbone is thought to occur at the rhamnose monosaccharides (Whitaker, 1984). Thus, the pectin found in processed citrus fiber is highly branched with relatively long side chains. Long galacturonic chains are known to promote both cross linking as well as gelling of pectin (Sila et al., 2009). Even though arabinose is not charged like galacturonic acid, the fact that there is such a large amount of the branches means it likely is another factor contributing to the rapid hydration properties (rate of hydration illustrated in *4.6 Morphology of citrus fiber*) of citrus fiber.

### 4.3. Rheology

Shear stress versus shear rate rheograms of the four different citrus fiber particle sizes show a nonlinear relationship between the shear stress and shear rate, especially at low shear rates and larger particle sizes, e.g. 400 μm (Fig. 1). At a smaller particle size, e.g. 12 μm (J01), there is less yield stress and the shape of the shear stress versus shear rate is closer to being linear. A larger particle size correlated with higher shear stress for any given shear rate

was observed, which is expected due to increased particle interactions with larger fiber length.

The model parameters for Herschel–Bulkley, Casson, Power Law, and Bingham Models along with the correlation coefficient ($R^2$) for each flow model are shown in Table 5. Based on the $R^2$ value, which model (Hershel–Bulkley, Casson, Power Law, and Bingham) has a good fit as a rheological model depends on the particle size of the fiber. As an example, for the sample with the biggest fiber length "F33", the Herschel–Bulkley model is the top ranked model with a $R^2$ of 0.974. The Herschel–Bulkley model predicts a yield stress and consistency coefficient of 2.50 Pa and 1.02 Pa s$^n$, respectively. Based on the $R^2$ value, the Casson model is the best fit for two samples, i.e. "A01" and "J01". In fact, because the Casson model fits two samples the best and also has a high $R^2$ for all the other samples as well, it is possibly the best ranking model and could be used to describe the flow behavior for any fiber length of citrus fibers within the range tested in this study. The Power Law model fits the sample "F27" the best, based on the $R^2$ value, but since this model does not exhibit a yield stress component, therefore, it does not seem like the best model to use. All the other models contain a yield stress component and they fit the samples other than the "F27" sample. The Bingham flow model has the highest $R^2$ value for Sample "A02", which is the second smallest particle size. The results from the Bingham model indicate that longer fibers tend to become increasingly non-Newtonian because the smaller fibers tend to have a high $R^2$ for this model while the longer fibers do not.

Through application of the rheological models, a trend of larger particle size correlated with higher yield stress was also observed. For example, if the Herschel–Bulkley model is used for all the analyses, the yield stress found was 2.5 Pa for the largest particle size and 0.39 Pa for the smallest particle size. Particles with longer fiber lengths and a higher aspect ratio tend to have a higher yield stress because of their greater interaction with one another. Thus, with a larger particle size, networks are easier to form which result in more particle interactions and thus, higher apparent viscosity and yield stress (Mueller et al., 2009).

In general, as fiber lengths get shorter and aspect ratios get smaller, they begin to act more like spherical particles in solution (Servais et al., 2002). Likewise, as fiber lengths get longer, they have more shear thinning-like behavior and thus, their flow index ($n$) is less than one (Mueller et al., 2009). The findings in this study were consistent with these theories and can be interpreted in couple different ways. First, the smallest particle size sample "J01" was found to have a flow index of 1.00 using the Herschel–Bulkley model whereas all the other larger sizes/lengths had a flow index less than one (Table 5). Also, when looking at the Bingham flow model data, where the flow index is fixed at one, the $R^2$ value of the model gets higher and shows a better fit to the data, as the particle sizes get smaller.

### 4.4. Apparent viscosity versus pH

The relationship between the apparent viscosity of citrus fiber (A02) and temperature is shown in Fig. 2. For this analysis, the solutions were prepared at pH 7 and 9 and then heated to the indicated temperature followed by immediate apparent viscosity measurement. At pH 7, the decrease in apparent viscosity was less affected by increasing temperature compared to other hydrocolloids. For instance, at 30 °C the apparent viscosity was 1470 cP, and at 70 °C, the apparent viscosity was 1056 cP, which was a 28% drop. This was different from more purified forms of hydrocolloids that tend to have a much more significant apparent viscosity drop with increasing temperatures, e.g. pectin had a three-fold apparent viscosity drop between the temperatures of 30 °C and 70 °C at a 3% concentration (Marcotte et al., 2001). The cellulose,

**Table 4**
Breakdown and analysis of the pectin monosaccharides contained in citrus fibers.

| Monosaccharide | Value (%) | $n$[a] | Std dev. (%) |
|---|---|---|---|
| Galacturonic acid | 23.30 | 4 | 1.12 |
| Degree of methylation (58.1%) | | 3 | 0.27 |
| Degree of acetylation (9.8%) | | 3 | 0.03 |
| Arabinose | 12.40 | 4 | 0.8 |
| Galactose | 4.14 | 4 | 0.36 |
| Rhamnose | 2.41 | 4 | 0.12 |
| Total Pectin | 42.25 | | |

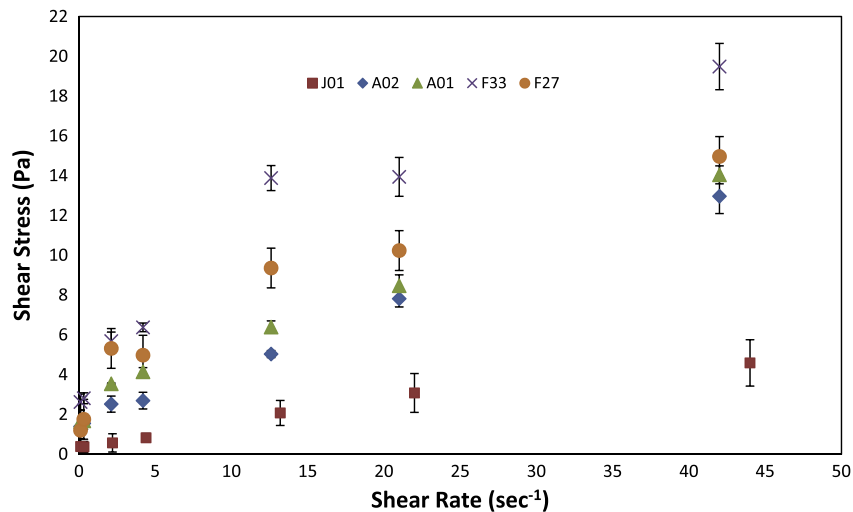[a] Indicates the number of measurements.

**Fig. 1.** Shear stress versus shear rate of 3% solutions of citrus fibers with various particle sizes. Error bars were calculated using a t-distribution with a 95% confidence interval.

**Table 5**
Rheological factors for 3% solutions of the various particle sizes of citrus fibers.

| Flow model | ID | $n$ | $K$ (Pa s$^n$) | Yield stress (Pa) | $R^2$ |
|---|---|---|---|---|---|
| Hershel Bulkley | F33 | 0.85 | 1.02 | 2.50 | 0.974[a] |
| | F27 | 0.80 | 0.93 | 1.55 | 0.898 |
| | A01 | 0.78 | 0.72 | 1.50 | 0.971 |
| | A02 | 0.78 | 0.58 | 1.30 | 0.994 |
| | J01 | 1.00 | 0.10 | 0.39 | 0.945 |
| Casson | F33 | – | 0.47 | 2.51 | 0.955 |
| | F27 | – | 0.43 | 1.62 | 0.932 |
| | A01 | – | 0.39 | 1.38 | 0.992[a] |
| | A02 | – | 0.39 | 0.96 | 0.989 |
| | J01 | – | 0.26 | 0.20 | 0.986[a] |
| Power Law | F33 | 0.35 | 4.77 | – | 0.962 |
| | F27 | 0.42 | 3.09 | – | 0.984[a] |
| | A01 | 0.36 | 2.90 | – | 0.955 |
| | A02 | 0.36 | 2.37 | – | 0.896 |
| | J01 | 0.43 | 1.52 | – | 0.884 |
| Bingham | F33 | – | 0.32 | 4.58 | 0.788 |
| | F27 | – | 0.30 | 3.29 | 0.893 |
| | A01 | – | 0.29 | 2.35 | 0.982 |
| | A02 | – | 0.28 | 1.62 | 0.996[a] |
| | J01 | – | 0.10 | 0.47 | 0.976 |

[a] these starred values indicate the highest $R^2$ model for the particular particle size.
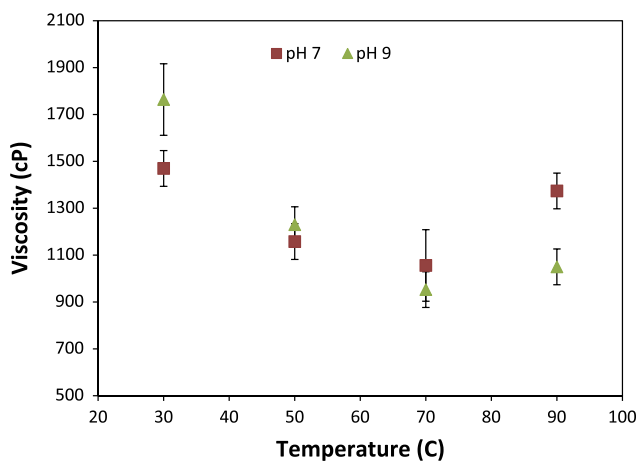


**Fig. 2.** Apparent viscosity of 3% solutions of citrus fiber (Sample "A02") at various temperature and pH. Error bars were calculated using a t-distribution with a 95% confidence interval.

and insoluble components in the citrus fiber help to stabilize the apparent viscosity while temperature increases. For instance, in a study with cellulose that was mechanically sheared, Chau et al. (2007) reported a minimal apparent viscosity change (9400–9500 cP) when the temperature increased from 25 °C to 50 °C at a 3% concentration. This apparent viscosity change of sheared cellulose with temperature is similar to the results obtained in this study, which is due to the insoluble components that are not heat-sensitive.

### 4.5. Water holding and swelling capacity

The water holding capacity and swelling capacity of citrus fiber with various particle sizes were measured to get an indication of the degree of hydrophilicity (Fig. 3). The reason for following the AACC 56-30 method was due to the partially soluble nature of citrus fiber, which can be lost in water holding capacity methods that discard the supernatant after centrifugation. In the second part of the AACC 56-30 method, various amounts of water were added to the sample in the centrifuge tube to see which water level had
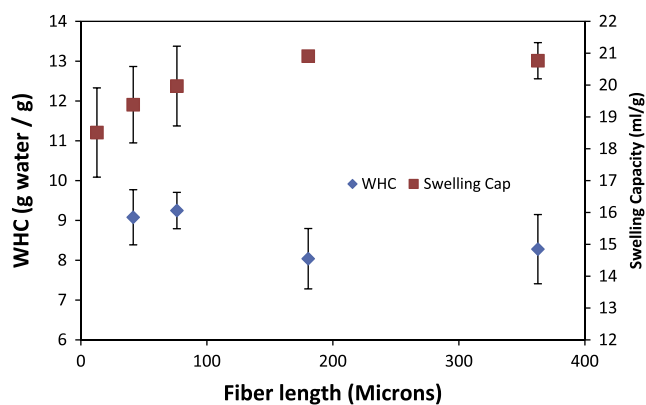
**Fig. 3.** Water holding capacity and swelling capacity of citrus fibers having various fiber lengths. The specific lengths and widths of the samples are shown in Table 1 ranging from Sample "J01" for the smallest size up to Sample "F33" for the largest size. Error bars were calculated using a t-distribution with a 95% confidence interval.

free water separation in order to ensure that the soluble components were retained. There was a small increase in the water holding capacity as particle size decreased (Fig. 3). With the increased water holding capacity it was necessary to use a smaller sample size to make sure there was enough water for the measurement.

In the swelling capacity analysis, there was no statistically significant difference (t-distribution, 95% confidence interval) between the particle sizes (Fig. 4). The average swelling capacity results reflect a small yet significant increase, e.g. 20%, as particle size increased from 12.7 µm up to 363 µm. However, even though the swelling capacity results were statistically significant, it is a small change.

Several studies reported different theories and results about why water holding capacity and swelling capacity vary for fibers depending on their size. One theory is that grinding adversely affects the water holding capacity because it results in a loss of the matrix structure while the packing density increases to create a lower water holding capacity during centrifugation or gravity settling (Kirwan et al., 1974). Results showing a decline in water holding capacity with smaller particle size have been reported in many studies (Cadden, 1987; Sangnark and Noomhorm, 2003; Mongeau and Brassard, 1982; Auffret et al., 1994). However, the theory proposed by Chau et al. (2007), which is relevant for citrus fibers, indicates that grinding to smaller particle size resulted in greater
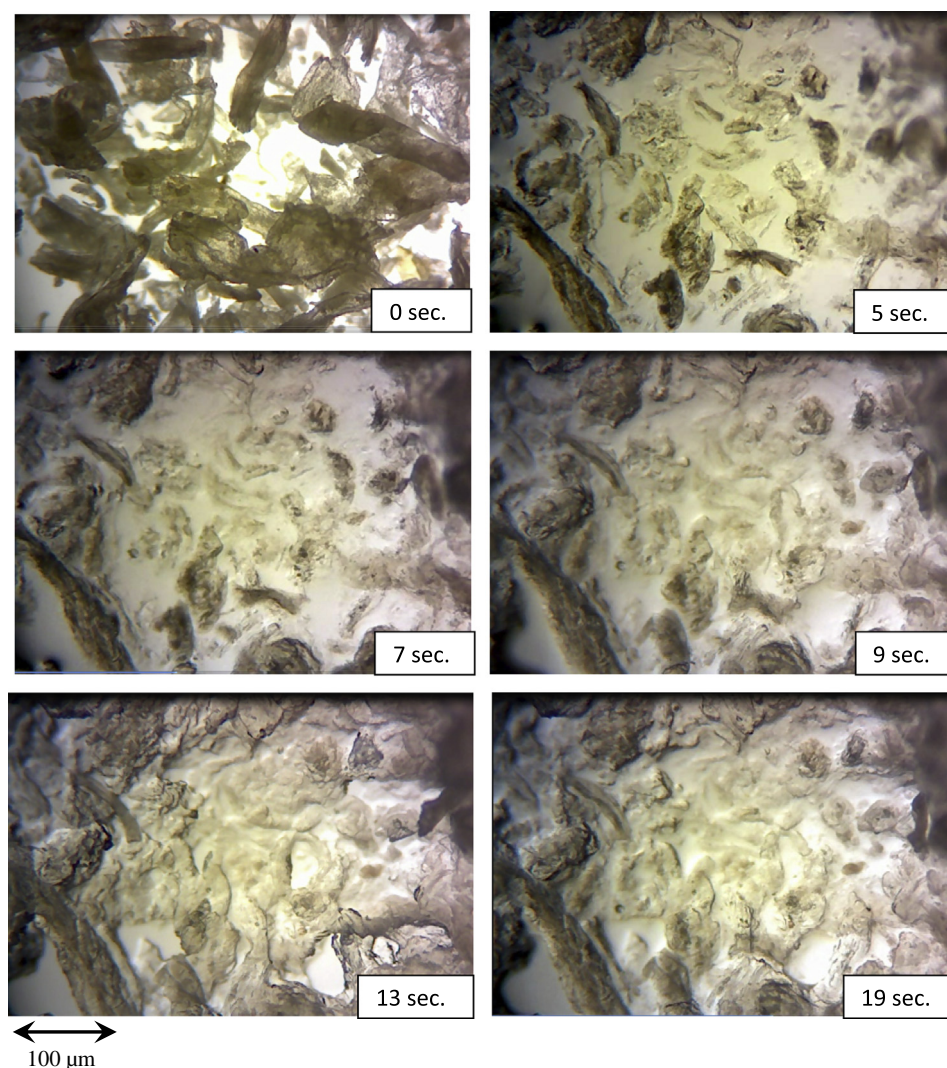


**Fig. 4.** Photos of citrus fiber "F33" before and after water is added to the fiber. Photos were taken at 37.5× magnification under a light microscope to illustrate effect of water causing the fiber structures to expand. The different times indicate the time after the water was added.

surface area and potential water binding sites and thus, led to an increase in the water holding capacity. Even though there is a relatively small difference in all the water holding capacity and swelling capacity results for the various particle sizes in this study, a possible explanation is that there are many competing forces off setting one another. For instance, on one hand there is a greater packing density with the smaller particle sizes, which works to reduce the water holding capacity, but on the other hand there is increased water-binding sites, polar groups, and surface area, which tends to result in increased water holding capacity.

### 4.6. Morphology of citrus fiber

Fig. 4 shows the impact of water on the structure of citrus fiber sample "F33". Dried citrus fiber is shown in the top right image (labeled as 0 s). The other photos reflect the amount of time after water was added, i.e. 5, 7, 9, 13, and 19 s. At 5 s, the fiber swells but many fiber structures are still clearly defined. At seven and 9 s, the more fibers swell and begin to lose some of their identity but there are still many voids present as not all the water is absorbed. However, at 13 and 19 s, nearly all the water appears to be absorbed into the fibers and there are minimal void spaces visible. At 13 and 19 s there are still fibrous structures visible but they lose their definition as the fibers are expanded and there appears to be both soluble and insoluble components, which would be consistent with the results found in the compositional analysis. Other than the very large particles that do not appear to swell, at 19 s the fibers are further swollen and appear to lose their individual identities and form an interconnected network of soluble and insoluble fibers.

This swollen network of fibers helps to illustrate and provide further understanding into the rheology and water holding capacity of the citrus fiber. For instance, the high water holding capacity and swelling capacity (Fig. 3) are the result of fibers absorbing water into their structures and expanding. In other words, the water is not merely bound on the surface of the fiber but rather gets absorbed into the fiber structure. The photos also help with the interpretation of the rheology results. For instance, the fibers clearly form a network that appear almost "gel-like", which would help explain the yield stress seen in the rheological models.

## 5. Conclusions

The composition, images, length/width, and rheological properties of citrus fibers in this study provide a much better understanding of the structure or form of citrus fibers and their functional properties. The rheological study can be used to improve how citrus fiber can be applied in food products to improve their quality and/or nutrition while maintaining or improving their taste profile. For instance, an important finding reported in this paper is the heat stability of citrus fibers over different pH values. This can be helpful in the creation of more heat stable food products. With regard to composition, pectin makes up approximately 42% of the citrus fiber composition, which is significant due to the largely insoluble nature of the fiber and the impact on water holding capacity. The hydration of citrus fibers can be better understood knowing the chemical composition.

The physical size of the citrus fibers has an important impact on apparent viscosity as well as the flow models used to describe its flow behavior. For instance, with a larger particle size the apparent viscosity and yield stress increased. The shape of the rheology curves also changed with particle size, and rheograms became more linear as the fiber length decreased. The Herschel–Bulkley model worked well to describe the citrus fibers with the largest fiber length. However, for the smaller fiber lengths the best fitting flow model varied. The Casson model seemed to work well with

a high correlation coefficient for all particle sizes analyzed in this project.

While the flow behavior changed depending on the fiber length, the water holding capacity did not appear to change with particle size. A theory was proposed that there are competing forces off setting one another. On one hand there is an increase in surface area that can hold additional water as fiber lengths are reduced but on the other hand there is a loss of the matrix structure, which also helps to hold water, as the fiber length decreased.

### Acknowledgments

### References

Auffret, A., Ralet, M.C., Guillon, F., Barry, J.L., Thaibault, J.F., 1994. Effect of grinding and experimental conditions on the measurement of hydration properties of dietary fibres. Lebensm. – Wiss. Technol. 27, 166–172.

Borwankar, R.P., 1992. Food texture and rheology: a tutorial review. J. Food Eng. 16 (1–2), 1–16.

Bourne, M.C., 1992. Food Texture and Viscosity. Academic Press, New York.

Braddock, R.J., 1983. Utilization of Citrus Juice Vesicle and Peel Fiber. Food Technol. 37 (12), 85–87.

Braddock, R.J., 1999. Handbook of Citrus By-Products and Processing Technology. John Wiley and Sons Inc., New York.

Cadden, A.M., 1987. Comparative effects of particle size reduction on physical structure and water binding properties of several plant fibers. J. Food Sci. 52 (6), 1595–1599.

Casson, N., 1959. A Flow Equation for Pigment-Oil Suspensions of the Printing Ink Type. Pergamon Press, London.

Charm, 1960. Viscometry of non-newtonian food materials. Food Res. 25, 351–362.

Chau, C.F., Wang, Y.T., Wen, Y.L., 2007. Different micronization methods significantly improve the functionality of carrot insoluble fibre. Food Chem. 100 (4), 1402–1408.

Garau, M.C., Simal, S., Rossello, C., Femenia, A., 2007. Effect of air-drying temperature on physico-chemical properties of dietary fibre and antioxidant capacity of orange (Citrus aurantium v. Canoneta) by-products. Food Chem. 104 (3), 1014–1024.

Grigelmo-Miguel, N., Martin-Belloso, O., 1999. Characterization of dietary fiber from orange juice extraction. Food Res. Int. 31 (5), 355–361.

Hartnett, J.P., Hu, R.Y.Z., 1989. The yield stress-an engineering reality. J. Rheol. 33, 671–679.

Kirwan, W.O., Smith, A.N., McConnel, A.A., Mitchell, W.D., Eastwood, M.A., 1974. Action of different bran preparations on colonic function. Br. Med. J. 4, 187–189.

Lundberg, B.M., 2005. Using highly expanded citrus fiber to improve the quality and nutritional properties of foods. Cereal Foods World 50 (5), 248–252.

Marcotte, M., Taherian, A.R., Ramaswamy, H.S., 2001. Rheological properties of selected hydrocolloids as a function of concentration and temperature. Food Res. Int. 34 (8), 695–703.

Mizrahi, S., Berk, Z., 1972. Flow behavior of concentrated orange juice: mathematical treatment. J. Texture Stud. 3, 69–79.

Mongeau, R., Brassard, R., 1982. Insoluble dietary fiber from breakfast cereal brans: bile salt binding and water holding capacity in relation to particle size. Cereal Chem. 59 (5), 413–417.

Mueller, S., Llewellin, E.W., Mader, H.M., 2009. The rheology of suspensions of solid particles. Proc. Royal Soc. 466 (21), 1202–1228.

Ofoli, R.Y., Morgan, R.G., Steffe, J.F., 1987. A generalized rheological model for inelastic fluid foods. J. Texture Stud. 18, 213–230.

Pimenova, N.V., Hanley, T.R., 2004. Effect of corn stover concentration on rheological characteristics. Appl. Biochem. Biotechnol. 114 (1), 347–360.

Raghavendra, S.N., Rastogi, N.K., Raghavendra, K.M., Tharanathan, R.N., 2004. Dietary fiber from coconut residue: effects of different treatments. Eur. Food Res. Technol. 218 (6), 563–567.

Rao, M.A., 1977. Rheology of liquid foods – a review. J. Texture Stud. 8, 135–168.

Ruan, R., Lun, J., Zhang, J., Addis, P., Chen, P., 1996. Structure-function relationships of highly refined cellulose made from agricultural fibrous residues. Appl. Eng. Agric. ASAE Publ. 12 (4), 465–468.

Sangnark, A., Noomhorm, A., 2003. Effect of particle sizes on functional properties of dietary fibre prepared from sugarcane bagasse. Food Chem. 80 (2), 221–229.

Saravacos, G.D., 1970. Effect of temperature on viscosity of fruit juices and purees. J. Food Sci. 35 (2), 122–125.

Servais, C., Luciani, A., Manson, J.E., 2002. Squeeze flow of concentrated long fibre suspensions: journal of non-newtonian fluid mechanics 104 (2), 165–184.

Sila, D.N., Buggenhout, S.V., Duvetter, T., Fraeye, I., Roeck, A.D., Loey, A.V., et al., 2009. Pectins in processed fruits and vegetables: part II – structure-function relationships. Compr. Rev. Food Sci. Food Safety 8 (2), 86–104.

Sluiter, A., Harnes, B., Ruiz, R., Scarlata, C., Sluiter, J., Templeton, D., et al., 2006. NREL Laboratory Analytical Procedure LAP #002: Determination of Structural Carbohydrates and Lignin in Biomass. National Renewable Energy Laboratory.

Steffe, J.F., 1996. Rheological Methods in Food Process Engineering. Freeman Press, East Lansing, MI.

Ting, S.V., 1970. Alchohol-insoluble constituents of juice vesicles of citrus fruit. J. Food Sci. 35 (6), 757–761.

Turbak, A.F., Snyder, F.W., Sandberg, K.R., 1983. Microfibrillated cellulose, a new cellulose product: properties, uses, and commercial potential. J. Appl. Polym. Sci.: Appl. Polym. Symp. 37 (2), 815–827.

Van Buren, J.P., 1979. The chemistry of texture in fruits and vegetables. J. Texture Stud. 10 (1), 1–23.

Waldron, K.W., Parker, M.L., Smith, A.C., 2003. Plant cell walls and food quality. Compr. Rev. Food Sci. Food Safety 2, 101–119.

Wen, L.F., Chang, K.C., Gallaher, D.D., 1998. Isolation and characterization of hemicellulose and cellulose from sugar beet pulp. J. Food Sci. 1 (1), 826–829.

Whitaker, J.R., 1984. Pectic substances, pectic enzymes and haze formation in fruit juices. Enzyme Microbiol. Technol. 6 (8), 341–349.

Willats, W.G., Knox, P., Mikkelsen, J.D., 2006. Pectin: new insights into an old polymer are starting to gel. Trends Food Sci. Technol. 17 (3), 97–104.

Yoo, S.H., Fishman, M.L., Savary, B.J., Hotchkiss, A.T., 2003. Monovalent salt-induced gelation of enzymatically deesterified pectin. J. Agric. Food Chem. 51 (25), 7410–7417.